2019 Rock Dynamics Summit– Aydan et al. (eds)
© 2019 Taylor & Francis Group, London, ISBN 978-0-367-34783-3

Model tests on rock slopes prone to wedge sliding and some case histories from recent earthquakes

H. Kumsar
Department of Geological Engineering, Pamukkale University, Dept. of Geological Engineering, Denizli, Turkey

Ö. Aydan
Department of Civil Engineering and Architecture, University of the Ryukyus, Okinawa, Japan

ABSTRACT: The wedge failure is one of the common forms of slope failures. In this study, the authors investigate the sliding responses of rock wedges under dynamic loads rather than the initiation of wedge sliding. Firstly some laboratory model tests are described. On the basis of these model tests on rock wedges, the theoretical model proposed previously is extended to compute the sliding responses of rock wedges in time domain. The proposed theoretical model is applied to simulate the sliding responses of rock wedge model tests and its validity is discussed. In the final part, the method proposed is applied to actual wedge failures observed in 1995 Dinar earthquake, 2007 Çameli earthquake and 2005 Pakistan-Kashmir earthquake, and the results are discussed.

1 INTRODUCTION

The stability of rock slopes under dynamic loading in mining and civil engineering depends upon the slope geometry, mechanical properties of rock mass and discontinuities, and the characteristics of dynamic loads with time (Aydan 2015). The wedge failure is one of the common forms of rock slope failures (Fig. 1).

In this study, the sliding responses of rock wedges under dynamic loads rather than the initiation of wedge sliding are investigated. Firstly some laboratory tests on model wedges are described. On the basis of these model tests on rock wedges, the theoretical models developed by Aydan and Kumsar (2010) are used to compute the sliding responses of rock wedges in time domain. In the final part, the method is applied to actual wedge failures observed in 1995 Dinar earthquake, 2007 Çameli earthquake and 2005 Pakistan-Kashmir earthquake, and the results are discussed.

2 DYNAMIC MODEL TESTS

2.1 *Preparation of Models*

Six special moulds were prepared to cast model wedges (Kumsar et al. 2000). For each wedge configuration, three wedge blocks were prepared. Each base block had dimensions of 140x100x260mm. Base and wedge models were made of mortar and their geomechanical parameters were similar to those of rocks.

The composition of the mortar used for the preparation of the models is 1781 kgf/m^3 of fine sand, 360 kgf/m^3 of cement with a water-cement ratio of 0.5. The cement used in mortar was rapid hardening type and samples were cured for about 7 days in a room with a constant temperature. The wedge angles and the initial intersection angles of wedge blocks are listed in Table 1.

In addition, several mortar slabs were cast to measure the friction angle of sliding planes. A number of tilting tests were performed. The inferred friction angle measured in tilting tests ranged between 30° and 34° with an average of 32°.

Figure 1. Some examples of wedge failure of rock slopes

Table 1. Geometric parameters of wedges (also see Figure 9).

Wedge Number	Intersection inclination - i_a (°)	Half-wedge Angle, ω_1=ω_2 (°)
TB1(Swedge120)	29	61.5
TB2(Swedge100)	29	51.5
TB3(Swedge90)	31	47.8
TB4(Swedge70)	27	40.0
TB5(Swedge60)	30	33.8
TB6(Swedge45)	30	26.0

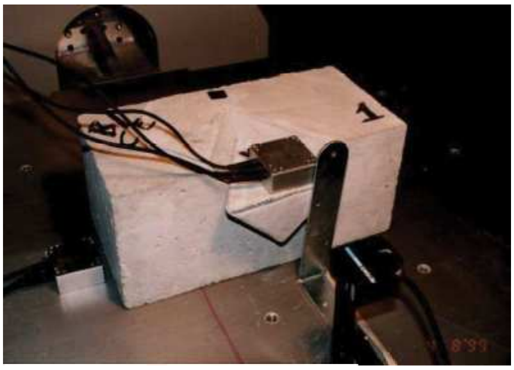

Figure 2. A view of a wedge model

Each wedge base block was fixed on the shaking table to receive same shaking with the shaking table during the dynamic test. The accelerations acting on the shaking table, at the base and wedge blocks were recorded during the experiment, and saved on a data file as digital data (Fig. 2). Furthermore, in the second series of dynamic tests, a laser displacement transducer was used to record the movement of the wedge block during the experiments. The reason for recording accelerations at three different locations is to determine the acceleration at the moment of failure as well as any amplification from the base to the top of the block. In fact, when the amplitude of input acceleration wave is increased, there is a sudden decrease on the wedge block acceleration records during the wedge failure, while the others are increasing. A barrier was installed at a distance of 20-30 mm away from the front of the wedge block to prevent their damage by falling off from the base block.

Dynamic testing of the wedge models were performed in the laboratory by means of a one-dimensional shaking table, which moves along horizontal plane. The applicable waveforms of the shaking table are sinusoidal, saw tooth, rectangular, trapezoidal and triangle. The shaking table has a square shape with 1m-side length. The frequency of waves to be applicable to the shaking table can range between 1 Hz and 50 Hz. The table has a maximum stroke of 100 mm and a maximum acceleration of 6 m/s^2 for a maximum load of 980.7 N.

2.2 *Shaking Table Tests*

Three experiments were carried out on each wedge block configuration and dynamic displacement responses of wedge blocks in addition to the acceleration responses were measured. Figs. 3-8 shows typical acceleration-time and displacement-time responses for each wedge block configuration. As it is noted from the responses shown in Figs. 3-8, the acceleration responses of the wedge block indicate some high frequency waveforms on the overall trend of the acceleration imposed by the shaking table. When this type waveform appears, the permanent

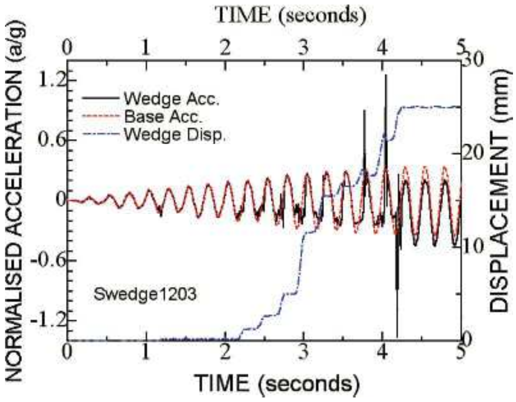

Figure 3. Dynamic response of Wedge Model TB1

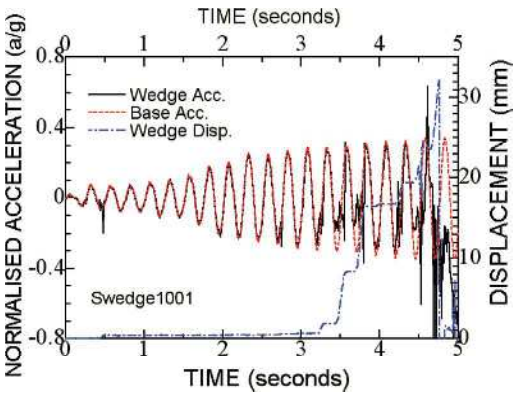

Figure 4. Dynamic response of Wedge Model TB2

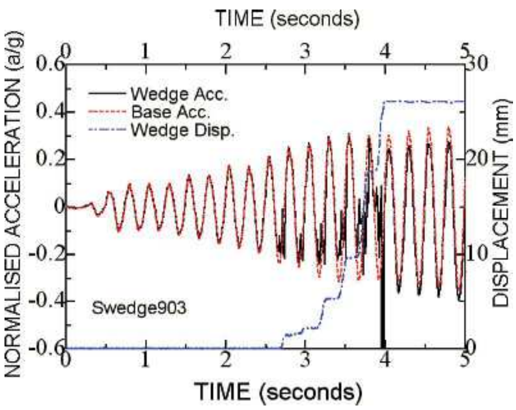

Figure 5. Dynamic response of Wedge Model TB3

displacement of the wedge block with respect to the base block takes place. Depending upon the amplitude of the acceleration waves as well as its direction, the motion of the block may cease. In other words, a step-like behavior occurs.

The motion of the block starts when the amplitude of the input wave acts in the direction of the

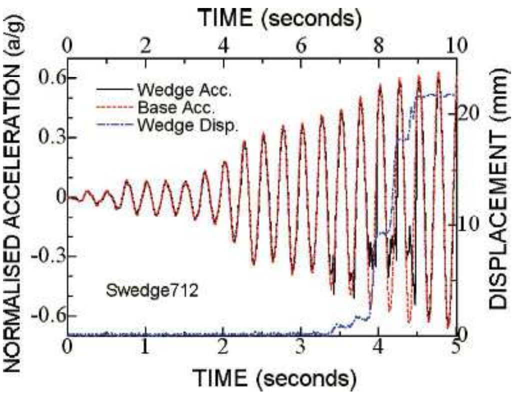

Figure 6. Dynamic response of Wedge Model TB4

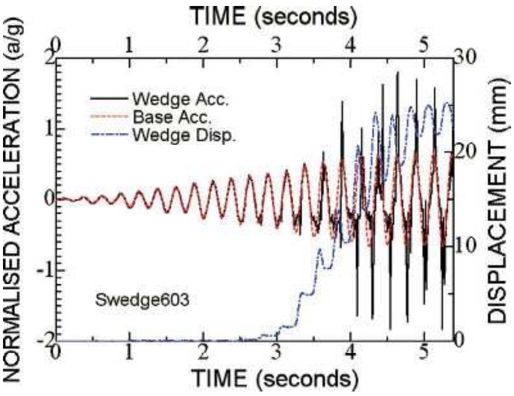

Figure 7. Dynamic response of Wedge Model TB5

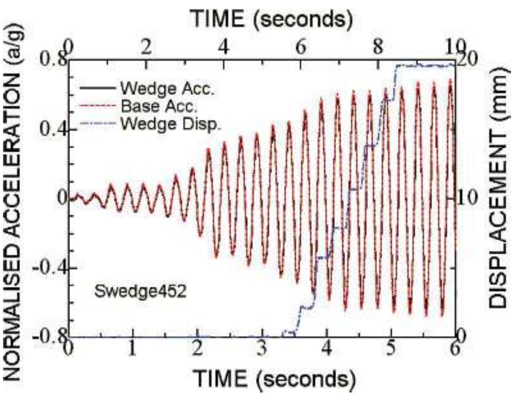

Figure 8. Dynamic response of Wedge Model TB6

downside and exceeds the frictional resistance of the wedge block. When the direction of the input acceleration is reversed, the motion of the block terminates after a certain amount of relative sliding. As a result, the overall displacement response is step-like.

Another important observation is that the frictional resistance between the wedge block and base-block limits the inertial forces acting on the wedge block and the base block even though the base-block may undergone higher inertial forces. The sudden jumps in the acceleration response of the wedge block as seen in Figs. 3-7 are due to the collision of the wedge block with the barrier. The initiation of the sliding of the wedge blocks was almost the same as those measured in the first series of the experiments.

3 THEORETICAL MODELLING

The authors have advanced the method of stability assessment proposed by Kovari and Fritz (1975) for wedge failure of rock slopes under different loading conditions and confirmed its validity through experiments (Kumsar et al. 2000). Aydan and Kumsar (2010) extended to evaluate sliding responses of rock wedges under dynamic loading conditions under submerged conditions with viscos resistance. Let us consider a wedge subjected to dynamic and water loading as shown in Figure 9. One can easily write the following dynamic equilibirum conditions for the wedge during sliding motion on two basal planes in a coordinate system *Osnp* shown in Fig. 9.

$$\sum F_s = (W - E_v)\sin i_a - E_i \cos i_a - S = m\frac{d^2 s}{dt^2} \quad (1)$$

$$\sum F_n = (W - E_v)\cos i_a - E_i \sin i_a - N = m\frac{d^2 n}{dt^2} \quad (2)$$

$$\sum F_p = -N_1 \cos\omega_1 + N_2 \cos\omega_2 + E_p = m\frac{d^2 p}{dt^2} \quad (3)$$

Where $N = N_1 \sin\omega_1 + N_2 \sin\omega_2$; W: weight of wedge; E_v: dynamic vertical load; E_i: dynamic force in the direction of intersection line; E_p: dynamic load

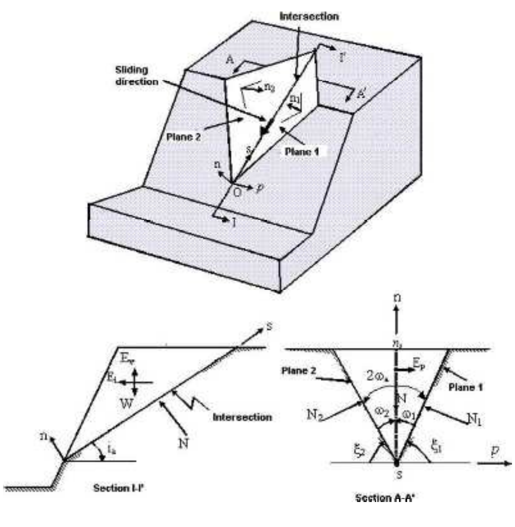

Figure 9. Illustration of mathematical model for wedge failure.

perpendicular to intersection line. Other parameters are shown in Fig. 9. Although the dynamic vectorial equilibirum equation are written in terms of its component, they correspond to a very general form for wedges sliding along the intersection line while being in contact with two basal planes. Furthermore, the earthquake force is decomposed to its corresponding components in the chosen coordinate system.

One can easily obtain the following identity from Eq.(3) by assuming that there are no motions upward and perpendicular to the intersection line:

$$N_1 + N_2 = \left[(W - E_v)\cos i_a - E_i \sin i_a\right]\lambda_i - E_p\lambda_p \quad (4)$$

Where

$$\lambda_i = \frac{\cos\omega_1 + \cos\omega_2}{\sin(\omega_1 + \omega_2)};\ \lambda_p = \frac{\sin\omega_1 - \sin\omega_2}{\sin(\omega_1 + \omega_2)} \quad (5)$$

If the resistance is assumed to obey Mohr-Coulomb criterion (Aydan and Ulusay, 2002; Aydan et al. 2008) one may write the following:

$$T = (N_1 + N_1)\mu\ ;\ \mu = \tan\varphi \quad (6a)$$

Following the initiation of sliding, the friction angle can be reduced to the kinetic friction angle as given below

$$\mu = \tan\varphi_r \quad (6b)$$

Where φ_r are residual cohesion and friction angle. Under frictional condition, it should be noted that normal force $(N_1 + N_2)$ can not be negative (tensile). If such a situation arise, normal force $(N_1 + N_2)$ should be set to 0 during computations. Let us introduce the following parameters:

$$\eta_v = \frac{E_v}{W} = \frac{a_v}{g};\ \eta_i = \frac{E_i}{W} = \frac{a_i}{g};\ \eta_p = \frac{E_p}{W} = \frac{a_p}{g} \quad (7)$$

where $a_v; a_i; a_p$ are acceleration components resulting from dynamic loading.

The following dynamic equilibrium equation must be satisfied during the sliding motion of the wedge.

$$S = T \quad (8)$$

If the relations given by equations (1),(4),(6),(7) are inserted in Eq. (8), one can easily obtain the following differential equation

$$\ddot{s} = \frac{d^2 s}{dt^2} = g\left[(1-\eta_v)A + \eta_i B + \eta_p C\right] \quad (9)$$

Where

$A = (\sin i_a - \cos i_a \mu\lambda_i)$; $B = (\cos i_a + \sin i_a \mu\lambda_i)$;
$C = \mu\lambda_p$

Since dynamic loads are very complex in time domain, the solution of Eq. (9) is only possible through numerical integration methods. The time-domain problems in mechanics are generally solved by finite difference techniques. For this purpose, there are different finite difference schemes. In this article the solution of Eq. (9) based on linear acceleration finite difference technique (i.e Aydan and Ulusay, 2002; Aydan et al. 2008). One can write the velocity ($\dot{s}$) and displacement of wedge (s) for a time step *n+1* as follows:

$$\dot{s}_{n+1} = \dot{s}_n + \frac{\ddot{s}_n}{2}\Delta t + \frac{\ddot{s}_{n+1}}{2}\Delta t \quad (10)$$

$$s_{n+1} = s_n + \frac{\dot{s}_n}{1}\Delta t + \frac{\ddot{s}_n}{3}\Delta t^2 + \frac{\ddot{s}_{n+1}}{6}\Delta t^2 \quad (11)$$

Provided that resulting dynamic shear force exceeds the shear resistance of the wedge at time $(t = t_i = i\Delta t)$, one can easily incorporate the variation of shear strength of discontinuities from peak state ($\mu = \tan\varphi_p$) to residual state ($\mu = \tan\varphi_r$).

4 COMPARISONS WITH EXPERIMENTS

The theoretical model presented in the previous section has been applied to experiments to compare the computed responses with those from experiments. Figs. 10 and 11 compare computational results for some of wedge blocks with measured sliding responses. The detailed comparisons for all wedge blocks are reported elsewhere (Aydan and Kumsar 2010). In computations, the peak friction angle of discontinuity planes reported in the previous publication (Kumsar et al. 2000) was reduced by 3° in order to take into account the slight damage to surfaces due to multiple utilization of wedge blocks. As noted from the measured and computed displacement responses, the results are remarkably similar to each other. Although some slight differences exist, these may be associated with the variation of the non-linear surface friction between the base-block and wedge block and the negligence of viscous effects in computations.

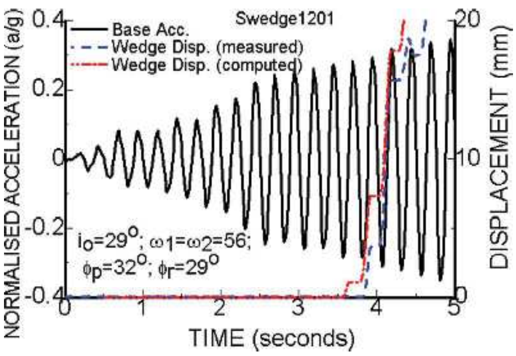

Figure 10. Comparison of computed responses with experimental response for TB1 wedge model.

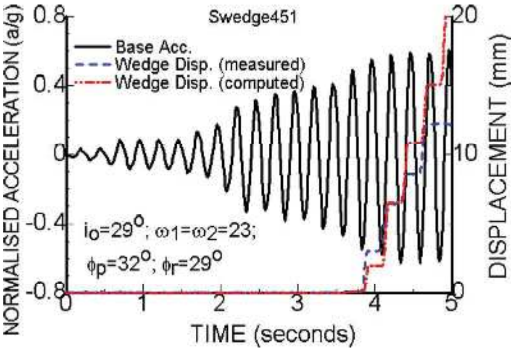

Figure 11. Comparison of computed responses with experimental response for TB6 wedge model.

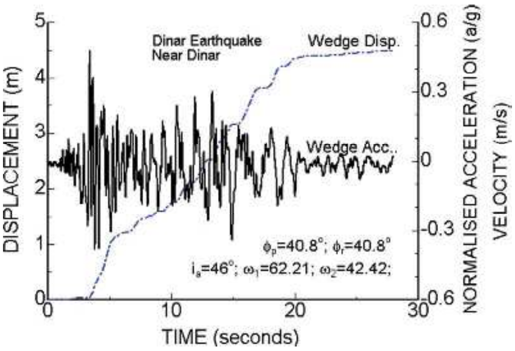

Figure 13. Computed displacement response of chosen wedge failure nearby Dinar.

5 APPLICATIONS TO WEDGE FAILURES CAUSED BY RECENT EARTHQUAKES

5.1 *Dinar Earthquake*

Dinar earthquake with a magnitude of 6.0 occurred on October 1, 1995 (Aydan and Kumsar, 1997). Many rock slope failures observed along the surface trace of the earthquake fault. At several locations on the eastern slope of the graben adjacent to the fault scarps, where the rock mass shows up, there were some rock slope failures. Rock mass is karstic conglomerate and bedding planes dip towards south with an inclination of 20°-25°. Most of rock slope failures were of small scale and associated with existing joints in rock mass. Slope failures were observed on eastern side of the graben next to Dinar-Çivril fault. The slope failures shown in Figure 12 were wedge failures nearby Dinar.

Tilting tests indicated that the friction angle of joint surfaces was about 40°. Fig. 13 shows the dynamic response of the wedge blocks nearby Dinar computed using the acceleration record obtained at Dinar strong motion station (DAD-ERD, 1995). As noted from the figure, wedge-sliding failure is initiated. Nevertheless, the motion terminates after a certain amount of displacement (4.5m). Such an amount of relative displacement was sufficient to displace the blocks and the blocks were fallen on the flatter ground as seen in Fig. 13.

Figure 12. Wedge failures nearby Dinar.

5.2 *The Kashmir Earthquake*

On October 8, 2005 at 8:50 (3:50UTC), a large devastating earthquake occurred in Kashmir region of Pakistan. The depth of the earthquake was estimated to be about 10 km and it had the magnitude of 7.6 (Aydan, 2006). The large slope failure occurred at Hattian (Dana Hill) and it was an asymmetric wedge sliding (Fig. 14). The wedge sliding failure at Hattian was quite large in scale. The sliding area was 1.5 km long and 1.0 km wide. Rock mass consisted of shale and sandstone and it constituted a syncline (Aydan et al. 2009). The estimated wedge angle was about 100° and it was asymmetric. The friction angle of shale from tilting test was more than 35° with an average of 40°.

The limiting equilibrium analysis for wedge sliding failure (Kumsar et al., 2000) indicated that the safety factor of the slope would be 1.55 under dry static conditions (Aydan and Kumsar, 2010). However, the mountain wedge becomes unstable when ground acceleration is equivalent to the horizontal seismic coefficient of 0.3 and the safety factor reduces to 0.9 under such a condition.

Using the acceleration record of Abbotabad (Ohkawa 2005) and multiplying the record by an

Figure 14. A view of Hattian slope failure.

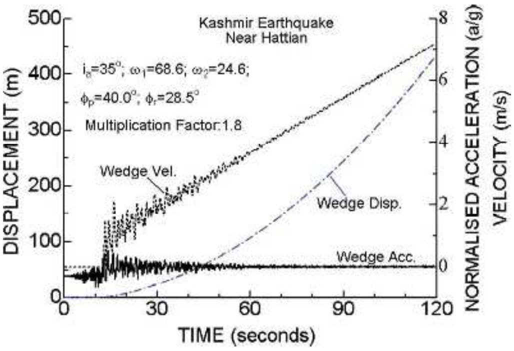

Figure 15. Computed displacement response of failed body of Hattian slope.

amplification factor of 1.27 so that the seismic coefficient value of 0.3 was achieved, a dynamic simulation of the wedge failure was carried out. The residual friction angle was reduced to 28.5° from the peak friction after yielding. The results are shown in Figure 15. The slope becomes unstable by the earthquake-induced ground shaking, the motion of the failed body increases with time.

Figure 16. A view of wedge failures at Taşçılar village.

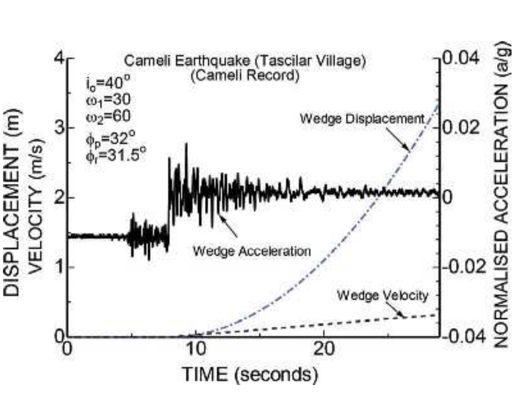

Figure 17. Computed displacement response of wedges failed at Taşçılar village due to the 2007 Çameli earthquake.

Unless the geometrical profile of the sliding surface changes, the sliding motion would continue with a constant velocity.

5.3 *The Çameli Earthquake*

The Çameli earthquake occurred at at 11:23 on TST (9:23 UTC) on October 29, 2007. The estimated magnitude of the earthquake varies between 4.9 and 5.4 depending upon the seismological institute. The earthquake caused some planar and wedge sliding failures in rock slopes consisting of marn. Figure 16 shows the computed dynamic response of the rock wedge for the assumed parameters shown in Figure 17. The wedge was assumed to be under dry conditions. As noted from the figure, the strong motion records taken at Çameli are sufficient to induce rock wedge sliding failure.

6 CONCLUSIONS

A series laboratory shaking table tests were carried on wedge models under dynamic excitations for the assessment of the validity of the limiting equilibrium method as well as to evaluate their sliding responses during shaking. The shaking table experiments on the wedge models were performed under dry conditions. Then, a method was presented to evaluate the dynamic sliding response of wedge blocks and the estimated sliding responses from the method presented were compared with experimental results. The results show that the estimated results are in a good agreement with the experimental results. In addition, the wedge failures induced by the 1995 Dinar earthquake, Çameli earthquake and the 2005 Kashmir earthquake were back analyzed and discussed. Although the wedge failures can be generally in small scale, it may sometimes be quite large in scale as observed at Hattian in Kashmir region of Pakistan.

REFERENCES

Aydan, Ö. (2006): Geological and Seismological Aspects of Kashmir Earthquake of October 8, 2005 and A Geotechnical Evaluation of Induced Failures of Natural and Cut Slopes. Journal of Marine Science and Technology, Tokai University, Vol.4, No.1, 25–44.

Aydan, Ö., (2015). Large Rock Slope Failures induced by Recent Earthquakes. Rock Mechanics and Rock Engineering, Special Issue on Deep-seated Landslides. 49(6),2503–2524.

Aydan, Ö. and H. Kumsar (1997). A site investigation of Oct. 1, 1995 Dinar Earthquake. Turkish Earthquake Foundation, TDV/DR 97–003.

Aydan, Ö., Ulusay, R. (2002): Back analysis of a seismically induced highway embankment during the 1999 Düzce earthquake. Environmental Geology, 42, 621–631.

Aydan, Ö., Kumsar, H. (2010). An Experimental and Theoretical Approach on the Modeling of Sliding Response of Rock Wedges under Dynamic Loading. Rock mechanics and Rock Engineering, Vol.43, No.6, 821–830.

Aydan, Ö., Ulusay R., Atak, V.O. (2008): Evaluation of ground deformations induced by the 1999 Kocaeli earthquake (Turkey) at selected sites on shorelines. Environmental Geology, Springer Verlag, 54, 165–182.

Aydan, Ö., Ohta, S., Hamada, M. (2009): Geotechnical evaluation of slope and ground failures during the 8 October 2005 Muzaffarabad Earthquake, Pakistan. Journal of Seismology 13(3),399-413. (DOI 10.1007/s10950-008-9146-7).

DAD-ERD, (1995). Earthquake Research Department of Turkey, http:www.deprem.gov.tr

Kovari, K., Fritz, P. (1975). Stability analysis of rock slopes for plane and wedge failure with the aid of a programmable pocket calculator. 16th US Rock Mech. Symp., Minneapolis, USA, 25–33.

Kumsar, H., Aydan, Ö. and Ulusay, R. (2000). Dynamic and static stability of rock slopes against wedge failures. Rock Mechanics and Rock Engineering, Vol.33, No.1, 31-51.

Okawa, I. (2005): Strong earthquake motion recordings during the Pakistan, 2005/10/8, http://www.bri.go.jp/